Enhancement of pulsed laser ablation in environmentally friendly liquid

Fangfang Luo,[1] Yingchun Guan,[2] Weili Ong,[1] Zheren Du,[1] Ghimwei Ho,[1] Fengping Li,[3] Shufeng Sun,[3] Gniancher Lim,[4] and Minghui Hong[1,*]

[1]*Department of Electrical and Computer Engineering, National University of Singapore, 4 Engineering Drive 3, Singapore 117576, Singapore*
[2]*School of Mechanical Engineering and Automation, Beihang University, 37 Xueyuan Road, Beijing 100191, China*
[3]*School of Mechanical and Electrical Engineering, Wenzhou University, Wenzhou 325035, China*
[4]*Singapore Institute of Manufacturing Technology, 71 Nanyang Drive, Singapore 638075, Singapore*
[*]*elehmh@nus.edu.sg*

Abstract: Enhancement of pulsed laser ablation can be achieved in acetic acid as an environmentally friendly liquid. This paper evaluates microholes and textured features induced by a nanosecond pulsed laser under different processing circumstances. The microholes are fabricated by laser drilling in acetic acid and found to be 100% deeper than in air. The textured features achieved in the liquid demonstrate a higher content of Copper and a lower content of Oxygen. The improvement of laser ablation efficiency in the liquid is attributed to the strong confinement of plasma plume accompanying with shockwave and cavitation bubbles. Meanwhile, the laser enhanced chemical etching by the weak acid plays a critical role.

OCIS codes: (140.3538) Lasers, pulsed; (240.6700) Surfaces.

References and links

1. A. M. Morales and C. M. Lieber, "A laser ablation method for the synthesis of crystalline semiconductor nanowires," Science **279**(5348), 208–211 (1998).
2. B. N. Chichkov, C. Momma, S. Nolte, F. V. Alvensleben, and A. Tünnermann, "Femtosecond, picosecond and nanosecond laser ablation of solids," Appl. Phys., A Mater. Sci. Process. **63**(2), 109–115 (1996).
3. A. Y. Vorobyev, V. S. Makin, and C. L. Guo, "Brighter light sources from black metal: significant increase in emission efficiency of incandescent light sources," Phys. Rev. Lett. **102**(23), 234301 (2009).
4. M. Huang, F. Zhao, Y. Cheng, N. S. Xu, and Z. Z. Xu, "Origin of laser-induced near-subwavelength ripples: interference between surface plasmons and incident laser," ACS Nano **3**(12), 4062–4070 (2009).
5. T.-H. Her, R. J. Finlay, C. Wu, S. Deliwala, and E. Mazur, "Microstructuring of silicon with femtosecond laser pulses," Appl. Phys. Lett. **73**(12), 1673–1675 (1998).
6. Y. C. Guan, G. K. L. Ng, H. Y. Zheng, M. H. Hong, X. Hong, and Z. Zhang, "Laser surface cleaning of carbonaceous deposits on diesel engine piston," Appl. Surf. Sci. **270**, 526–530 (2013).
7. J. Yang, F. F. Luo, T. S. Kao, X. Li, G. W. Ho, J. H. Teng, X. G. Luo, and M. H. Hong, "Broadband ultra-low reflectivity black Si surfaces: design and fabrication by laser micro/nanoprocessing," Light: Sci. Appl. **3**(1), e185 (2014).
8. M. E. Shaheen, J. E. Gagnon, and B. J. Fryer, "Femtosecond laser ablation of brass in air and liquid media," J. Appl. Phys. **113**(21), 213106 (2013).
9. N. Krstulović, S. Shannon, R. Stefanuik, and C. Fanara, "Underwater-laser drilling of aluminum," Int. J. Adv. Manuf. Technol. **69**, 1765–1773 (2013).
10. J. Lu, R. Q. Xu, X. Chen, Z. H. Shen, X. W. Ni, S. Y. Zhang, and C. M. Gao, "Mechanisms of laser drilling of metal plates underwater," J. Appl. Phys. **95**(8), 3890–3894 (2004).
11. W. D. Song, M. H. Hong, B. Lukyanchuk, and T. C. Chong, "Laser-induced cavitation bubbles for cleaning of solid surfaces," J. Appl. Phys. **95**(6), 2952–2956 (2004).
12. S. Zhu, Y. F. Lu, and M. H. Hong, "Laser ablation of solid substrates in a water-confined environment," Appl. Phys. Lett. **79**(9), 1396–1398 (2001).
13. A. V. Simakin and G. A. Shafeev, "Laser-assisted etching-like damage of Si," Appl. Surf. Sci. **86**(1-4), 422–427 (1995).
14. M. R. Brook and G. A. Shafeev, "Laser-assisted engraving of HgCdTe under a liquid layer," Appl. Surf. Sci. **54**, 336–340 (1992).
15. M. H. Hong, K. Y. Ng, Q. Xie, L. P. Shi, and T. C. Chong, "Pulsed laser ablation in a cooled liquid environment," Appl. Phys., A Mater. Sci. Process. **93**(1), 153–157 (2008).
16. J. M. Lee and K. G. Watkins, "Laser removal of oxides and particles from copper surfaces for microelectronic fabrication," Opt. Express **7**(2), 68–76 (2000).

#213369 - $15.00 USD Received 3 Jun 2014; revised 2 Sep 2014; accepted 3 Sep 2014; published 23 Sep 2014

17. M. Y. Shen, C. H. Crouch, J. E. Carey, and E. Mazur, "Femtosecond laser-induced formation of submicrometer spikes on silicon in water," Appl. Phys. Lett. **85**(23), 5694–5696 (2004).
18. B. Kumar and R. K. Thareja, "Laser ablated copper plasmas in liquid and gas ambient," Phys. Plasmas **20**(5), 053503 (2013).
19. B. Kumar and R. K. Thareja, "Growth of titanium nanoparticles in confined plasma," Phys. Plasmas **19**(3), 033516 (2012).
20. M. Aghaei, S. Mehrabian, and S. H. Tavassoli, "Simulation of nanosecond pulsed laser ablation of copper samples: A focus on laser induced plasma radiation," J. Appl. Phys. **104**(5), 053303 (2008).
21. Y. L. Liao, Y. L. Yang, and G. J. Cheng, "Enhanced laser shock by an active liquid confinement—hydrogen peroxide," J. Manuf. Sci. Eng. **134**(3), 034503 (2012).
22. K. J. Laidler, *The World of Physical Chemistry* (Oxford University Press, 1993).
23. H. B. Zeng, W. P. Cai, Y. Li, J. L. Hu, and P. S. Liu, "Composition/structural evolution and optical properties of ZnO/Zn nanoparticles by laser ablation in liquid media," J. Phys. Chem. B **109**(39), 18260–18266 (2005).

1. Introduction

In recent decades, pulsed laser ablation has attracted considerable attentions from not only the theoretical studies of laser-matter interactions but also the practical industrial applications [1–7]. Laser ablation is a complex physical and chemical process, which consists of laser induced carrier excitation, plasma formation, photothermal transformation and photochemical reaction. These interactions result in various surface features, including microholes [2], micro/nano-ripples [3, 4] and microspikes [5]. To achieve high laser ablation efficiency is a key objective for its practical applications. The most common method is to optimize laser processing parameters, such as light wavelength, laser fluence, pulse width and repetition rate [2–6]. Nowadays, research has shown more interests in hybrid approaches by changing processing environment from ambient air to liquid. Many types of liquids, such as water, ethanol, isopropanol and acetone, have been applied to assist laser ablation [8–12]. Results show that laser ablation in liquids induces plasma plume with a higher temperature and pressure as well as a stronger shockwave with a longer duration and a higher impact force, compared with that in ambient air. It increases the efficiency of material removal. Moreover, the fluidity of liquid results in a further removal of the ablated debris with clean ablation edges. However, previous works mostly focus on neutral liquids, which do not cause any chemical reaction between the liquid and substrate during the laser irradiation.

It is well known that when a metal immerses inside a strong acid or alkali liquid, the metal reacts intensively with the liquid and its surface layer is easily removed. Correspondingly, it is possible that the laser ablation can be enhanced with an assist of these liquids [13–15]. Unfortunately, such strong liquids are harmful to the environment. Moreover, the ablation speed is also hard to control, and undesired background etching happens on the sample surface. Therefore, it is necessary to investigate the effect of laser ablation in a weak acid or alkali liquid, which is environmentally friendly for green manufacturing.

In this paper, we study the effect of acetic acid, an environmentally friendly liquid, on the laser ablation of copper (Cu) substrates. Two types of laser ablation, drilling and texturing, are carried out. Laser drilling is to make microholes, and laser texturing is to achieve large-area surface modification. These two laser ablation processes demonstrate that it can be improved with an assist of the acetic acid. This improvement is attributed to the strong confinement of plasma plume as well as the localized chemical etching of the substrate materials done by the acetic acid, which is confined at the high temperature region defined by the laser interactions with materials.

2. Experimental

Copper foils covered with a thin layer of copper oxide (CuO and Cu_2O) were used as samples. Cu has important applications in printed circuit boards, integrated circuits and artifacts [16]. However, it is easily oxidized due to the unpaired outermost electrons. Coppers stored in ambient atmosphere are attached by a thin layer of copper oxide. For the better practical applications, it is a need to investigate the effect of laser ablation on the bulk copper with a layer of oxidation, instead of the pure copper. The Cu foils was firstly cut into a dimension of $40 \times 30 \times 1$ mm^3 and then cleaned in acetone and DI-water. After drying, the samples were

#213369 - $15.00 USD Received 3 Jun 2014; revised 2 Sep 2014; accepted 3 Sep 2014; published 23 Sep 2014

baked in an oven at 300℃ for 8 minutes. Subsequently, the color of the samples changed from a shiny surface to dark brown, which indicated a layer of copper oxide being formed and attached onto the sample surfaces.

A 1064 nm pulsed fiber laser was employed for the laser ablation, operating at a pulse width of 10 ns, a repetition rate of 10~100 kHz, and a maximum pulse energy at 1.8 mJ. The laser pulses were focused via an objective (10 × , NA = 0.3) or an F-theta lens at a focusing length of 100 mm onto the sample surface. Acetic acid was a mixture of DI-water and commercial vinegar bought from a supermarket for household usage. The vinegar was eco-friendly and inexpensive. The volume ratio of DI-water and vinegar was 25:1 and the PH of the mixture was measured as 2.9. Laser ablation in air and DI-water was also carried out for comparison. The depth of the liquid, from liquid surface to the sample top surface, varied from 1 to 4 mm. The technique of the laser drilling and multi-scanning was employed to investigate the effect on the material removal. After the laser processing, the samples were cleaned by DI-water and dried for measurement. A scanning electron microscope (SEM) was used to determine the surface morphology of the treated samples. An atomic force microscopy (AFM) was used to determine the 3-Dimensional surface morphology and roughness of the treated surfaces. A surface profilometer was used to measure its profile. The elemental analysis was carried out by an energy-dispersive X-ray spectroscopy (EDX).

3. Results and discussion

Figures 1(a)-1(c) show the SEM images of the microholes made by the laser drilling, and Figs. 1(d)-1(f) show the 2-D profile of the microholes in Figs. 1(a)-1(c), respectively. The samples were irradiated by 400 laser pulses at a laser fluence of 10 J/cm^2 in air, acetic acid and DI-water. For the drilling in air, a microhole has a diameter of 8 ± 0.7 μm and its rim with redeposited materials is higher than the unaffected surrounding area as shown in Figs. 1(a) and 1(d). While for the drilling in the acetic acid, the formed microhole shows different features. As shown in Figs. 1(b) and 1(e), there is no redeposited material around the microhole, and the rim of the microhole has the same height as the surrounding area. Moreover, the diameter of the microhole is 30 ± 1.5 μm, around 4 times of that in Fig. 1(a). The features of the microholes formed in DI-water are similar to those in acetic acid as shown in Figs. 1(c) and 1(f). It can be concluded that the laser ablation with an assist of liquid results in a significant increase of material removal and better laser processing quality compared to that in air.

Figure 2 shows that the depth varies with pulse number in air, acetic acid and DI-water. The laser fluence was fixed at 10 J/cm^2 and the pulse number changed from 50, 80, 100, 200, 400, 600, 800 to 1000. The thickness of the acetic acid and DI-water above the samples was set to be 1, 2, 3 and 4 mm, respectively. A group of 5 microholes was drilled by each laser processing parameter. The arithmetic average and standard error of the measured depth of each group are shown in Fig. 2. It can be seen that the microholes are deeper in the acetic acid than in DI-water and air. For example, with an exposure of 400 pulses, the depth of the microholes in the acetic acid at a liquid thickness of 2 mm is 51 ± 1.3 μm, while it is 47 ± 1.6 μm in Di-water and 25 ± 1.1 μm in air, as shown in Fig. 1. The depth of microholes is also found to change with the liquid thickness in Fig. 2. The maximum depth in the acetic acid reaches at a thickness of 2 mm, and the maximum depth in DI-water is 3 mm. An optimal

#213369 - $15.00 USD Received 3 Jun 2014; revised 2 Sep 2014; accepted 3 Sep 2014; published 23 Sep 2014

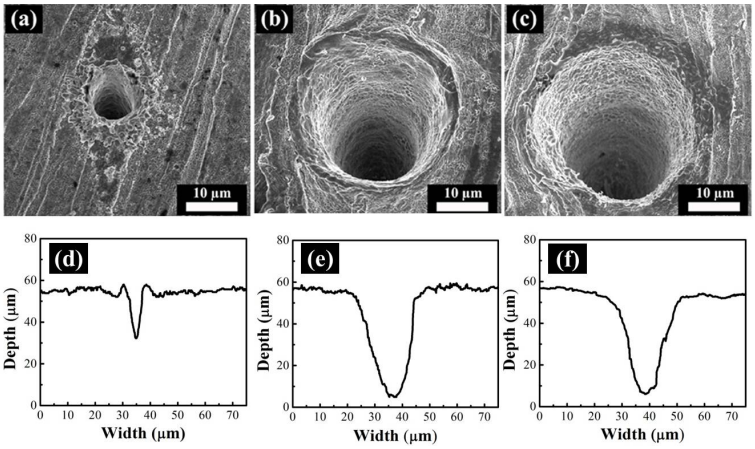

Fig. 1. SEM images of microholes on Cu samples formed by laser drilling in different environments of (a) air, (b) acetic acid, and (c) DI-water. Microholes produced by the fiber laser drilling at a laser fluence of 10 J/cm^2 and a pulse number of 400. 2-D profiles of the microholes in Figs. 1(a)-1(c) are shown in Figs. 1(d)-1(f). (The samples are tilted at 15° for taking SEM images.)

depth of liquid thickness for the microhole growth results from the balance between the pressure confinement and the absorption of the incident laser in liquid [9]. On one hand, the thicker liquid results in a higher confinement for the laser induced plasma. This confinement results in a better growth of shock wave and cavitation bubbles, leading to the improvement of the material removal and the ablation rate. On the other hand, the greater depth of the liquid causes a bigger loss of laser energy irradiating on the sample surface due to a higher absorption. Thus, the plasma plume with lower pressure and temperature takes place and laser ablation is weakened.

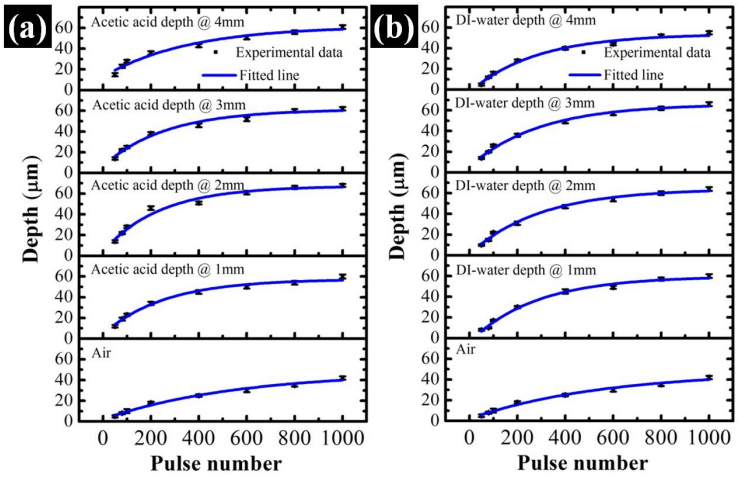

Fig. 2. Depth evolution of the microholes with pulse number and liquid thickness drilled in (a) acetic acid and (b) DI-water. The results in air are presented as a reference. The pulse number is set as 50, 80, 100, 200, 400, 600, 800 and 1000, respectively.

To further investigate the liquid enhancement of the laser ablation, a high speed scanning approach was employed for large-area ablation on the sample surface. The laser repetition rate was set to be 100 kHz and laser fluence was 1 J/cm^2. The scanning speed was fixed at 200 mm/s. To achieve the optimal ablation, the acetic acid thickness of 2 mm and water thickness of 3 mm were employed to assist the laser processing. The SEM images of the sample

#213369 - $15.00 USD Received 3 Jun 2014; revised 2 Sep 2014; accepted 3 Sep 2014; published 23 Sep 2014

surfaces before and after the laser processing in air, acetic acid and DI-water are shown in Fig. 3. There are two different features among these textured surfaces. One is the size of micro/nanoprotrusions developed on these surfaces. It can be seen that the micro/nanoprotrusions developed in air (as shown in Fig. 3(b)) is thicker than those in acetic acid and DI-water (in Figs. 3(c) and 3(d)). The other is the presence of nanoparticles on the surfaces processed in acetic acid and DI-water while nearly no nanoparticles can be found on the textured surfaces in air. Figure 4 shows the AFM images of copper surfaces before and after the laser processing in air, acetic acid and DI-water. The measured areas of Figs. 4(a)-4(d) are corresponding to those of Figs. 3(a)-3(d). The average roughness of the surfaces of Figs. 4(a)-4(d) is 27 ± 5, 114 ± 8, 174 ± 16 and 195 ± 14 nm, respectively. This demonstrates that the existence of the micro/nanostructures makes the surfaces rougher.

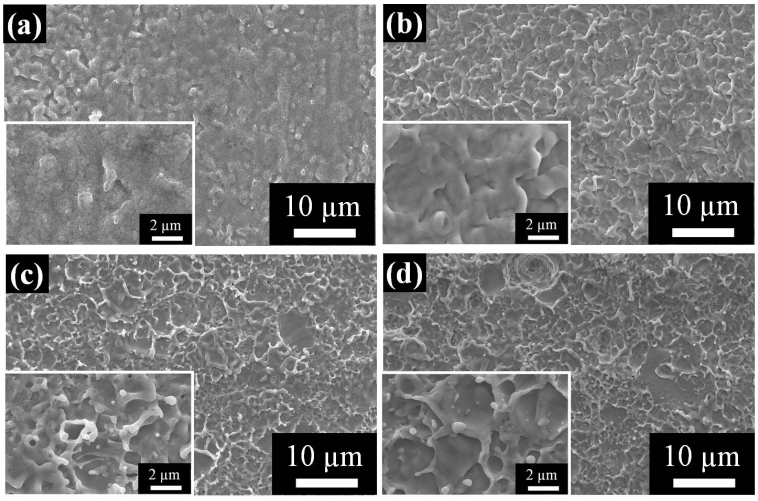

Fig. 3. SEM images of Cu surfaces (a) before and after the laser ablation in (b) air, (c) acetic acid, and (d) DI-water. The sample surfaces treated by the fiber laser at a speed of 200 mm/s and laser fluence of 1 J/cm^2.

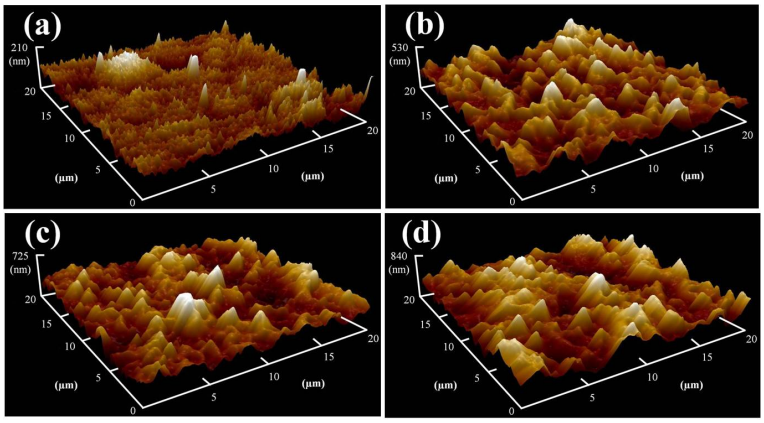

Fig. 4. AFM images of copper surfaces (a) before and after the laser ablation in (b) air, (c) acetic acid, and (d) DI-water. The measured areas of Figs. 4(a)-4(d) are corresponding to those of Figs. 3(a)-3(d).

The difference in the size of the micro/nanoprotrusions can be explained by the higher pressure of the surrounding confinement plasma and more effective cooling effect in the liquid medium [17–19]. The generation of micro/nanoprotrusions results from the solidification of the molten materials under the plasma plume induced by the irradiated laser

#213369 - $15.00 USD Received 3 Jun 2014; revised 2 Sep 2014; accepted 3 Sep 2014; published 23 Sep 2014

[17]. The generation of the plasma plume will be illustrated in detail in the latter part. Under the liquid ambient, the expansion of the plume is strongly confined by the higher density of the liquid. Meanwhile, due to the higher heat capacity and thermal conductivity of the liquid, the plasma plume cools down much faster than in air. It is reported that the electron temperature of the copper plasma in the liquid is estimated to be ~5800 K at a time delay of 300 ns, which is a half of that in air [18]. These factors result in a smaller molten area under the plume in the liquid. The rapid cooling process of the molten area also makes slimmer protrusions on the surface in the liquid than in air. Therefore, the protrusions developed in the liquid have a smaller size than in air. On the other hand, some of the molten areas are squeezed and pushed aside by the strong shock wave in the liquid, leaving behind the microcraters on the surface. The existing of these microcraters results in a higher roughness of the surfaces as shown in Fig. 4.

Figure 5 shows the elemental analysis of the copper surfaces after laser texturing by changing the scanning times from 1 to 9 in air, acetic acid and DI-water. It can be seen that the concentrations of O and Cu at the textured surfaces change with the processing conditions. The concentration of O for the ablation in the acetic acid is lower than that in air and DI-water (Fig. 5(a)), while the concentration of Cu in the acetic acid is higher than that in air and DI-water (Fig. 5(b)). Moreover, with the increase of scanning times, the concentration of O decreases while the concentration of Cu increases. When the scanning times increases to 9, the concentration of O in the acetic acid reaches a minimum value of (1.53 ± 0.26)%, while the concentrations of O in the DI-water and air accounts for (3.63 ± 0.36)% and (10.62 ± 0.38)%, respectively. Compared to the processing in air and DI-water, laser ablation in the acetic acid is more effective to remove the layer of the surface oxide.

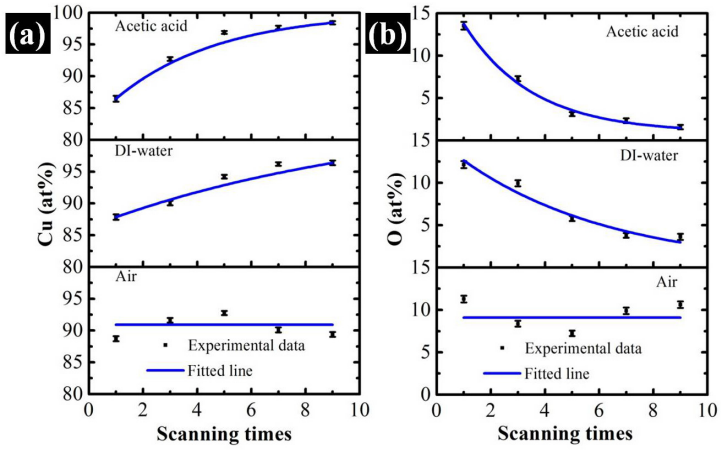

Fig. 5. EDX elemental analysis of the samples at different processing conditions, (a) Copper (at%) and (b) Oxygen (at%).

Enhancement of pulsed laser ablation in the acetic acid is attributed to the strong confinement of the plasma plume and the assisted localized chemical etching [17–21]. When a laser beam at a high intensity is focused on the sample surface, the electrons are heated and excited to high-excited states due to inverse-bremsstrahlung process [20]. Followed by electron-neutral or electron-ion collisions and energy transfer, a dense cloud of ions and atoms in excited state, such as Cu^{2+}, Cu^{+}, O^{2-} and Cu*, are ignited [21]. The plasma plume then develops to a mixture vapour containing these ions, atoms and electrons, as shown in Fig. 6(a). With the continued absorption of the later part of laser pulse energy, the formed plasma plume experiences an isothermal expansion, and the pressure and temperature increase at a relatively high speed, as shown in Fig. 6(b). After the laser pulse terminates, the plasma plume adiabatically expands as shown in Fig. 6(c) and is characterized by high pressure and high temperature. The pressure of the plasma plume was demonstrated to be a few gigapascals

#213369 - $15.00 USD Received 3 Jun 2014; revised 2 Sep 2014; accepted 3 Sep 2014; published 23 Sep 2014

and the temperature can reach up to thousands of Kelvin [19]. This expansion lasts for around 100 μs and then shrinks up to collapse. Under this extreme condition, the ions, including CH_3COO^- and H^+, speed up around the plasma plume. Therefore, the chemical reactions at the liquid-plasma interface take place as follows,

$$CH_3COOH + CuO \rightarrow (CH_3COO)_2\,Cu + H_2O, \text{ or} \quad (1)$$

$$CH_3COOH + Cu_2O \rightarrow CH_3COOCu + H_2O. \quad (2)$$

More importantly, the reaction rate of these reactions is accelerated due to the high temperature around the plasma induced by the laser irradiation. Arrhenius proposed a simple equation for the dependence of the rate k of a chemical reaction on the absolute temperature T [22],

$$k = A\exp\left(-Ea/(k_B T)\right) \quad (3)$$

where A is the pre-exponential factor, Ea the activation energy, and k_B the Boltzmann constant. Equation (3) reveals that the rate constant k is an exponential multiplied by temperature T. It means that the reactions (1)-(2) are much intensive at a higher temperature. On the other hand, due to extreme conditions around the plasma, thermal evaporation and decomposition of molecules, including CH_3COOH and H_2O, are excited, resulting in the generation of cavitation bubbles. The shock wave with a strong force is induced as a result of the energetic expansion of the plasma plume. The plasma plume condensates into clusters and aggregates into nanoparticles [23]. The subsequent removal of nanoparticles by shock wave and cavitation bubbles results in the material removal from the irradiation area.

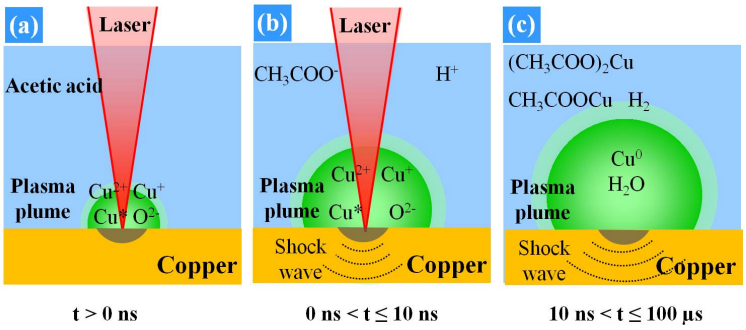

Fig. 6. Schematic illustration of the laser processing in the acetic acid. (a) the plasma plume is ignited on the irradiated spot, (b) the plasma plume isothermally expands by the absorption of laser energy, (c) after the laser pulse terminates, the plasma plume adiabatically expands and chemical reaction takes place at the liquid-material interface.

Based on the discussion above, the enhancement of the pulsed laser ablation in the acetic acid can be interpreted. When the samples is drilled in the acetic acid by the multiple pulses of laser ablation, the induced shock wave and cavitation bubbles with a strong force drive intensively nanoparticles and also the melted materials away from the irradiated area. Moreover, the chemical reaction around the irradiated area further increases the removal of target materials. Therefore, the depth of drilling holes is much deeper in the acetic acid than that in Di-water and air. For the laser texturing, the ablation modifies the local surface around the irradiated area. When the laser irradiates on the material surface, one part of laser energy excites the plasma plume and the rest is convertible to thermal energy into the target surface, resulting in a layer of molten material on the surface. In case of the acetic acid ambient, the oxidations on the molten surfaces, CuO and Cu_2O, actively react with CH_3COOH because of the thermal ionization as mentioned above. Due to the abundance of H^+ ions, the O^{2-} ions from photolysis and thermolysis are prior in combination with H^+ ions. Therefore, most of the Cu^{2+} and Cu^+ ions lose the chance to recombine with O^{2-} ions, and exists in the form of Cu^0

#213369 - $15.00 USD Received 3 Jun 2014; revised 2 Sep 2014; accepted 3 Sep 2014; published 23 Sep 2014

atoms due to the photonic reduction or $(CH_3COO)_2Cu$ or CH_3COOCu in acetic acid. As a result, the removal of the oxidation layer is easier to achieve in the acetic acid than that in air and DI-water. Moreover, the bare Cu substrate is not easy to be oxidized because of scarcity of O^{2-} ions. Therefore, the concentration of O on the material surfaces processed in the acetic acid is lower than that in air and DI-water, and the concentration of Cu in the acetic acid is higher than that in air and DI-water.

4. Conclusion

The laser ablation of copper substrates can be greatly improved by immersing the samples inside environmentally friendly liquid of the acetic acid. For the laser drilling, the depth of induced microholes in the acetic acid is twice of that in air. For the laser texturing, the elemental analysis indicates that the laser treated areas in the acetic acid show a higher content of Cu and a lower content of O compared to that in air. The improvement of the laser ablation is attributed to the strong confinement of plasma plume and the accompanying shockwave and cavitation bubbles. Moreover, the chemical reaction between the target materials and the liquid plays an important role. The laser processing in the acetic acid offers an effective and environmentally friendly means to enhance material removal as well as surface clean during the laser ablation.

Acknowledgments

This work was supported by A*STAR Remanufacturing Program with project code U11-M-030AU, Temasek Defence Systems Institute (TDSI) with project No. R-263-000-687-592 TDSI/11-013/1A, and Science Technology Department of Zhejiang Province, China (Project No. 2012C14026).